Investigation of the Effect of Titanium Dioxide and Aluminum Titanate on Physical, Mechanical, and Microstructural Properties of Synthesized Cordierite

Amir Hojjati Lemraski [a, b], Ali Sedaghat Ahangari Hossein Zadeh [a,*], Rahim Naghizadeh [b], Hudsa Majidian [a]

[a] Department of Ceramic, Materials and Energy Research Center, Karaj, Iran

[b] Iran University of Science and Technology, School of Metallurgy and Materials Engineering, Narmak, Tehran 16846–13114, Iran

[*]Corresponding author; E-mail address: a.sedaghat@merc.ac.ir

Abstract

Cordierite ceramics are of interest for various applications due to their properties such as low thermal expansion coefficient and high thermal shock resistance. However, due to the narrow range of sintering temperature, attempts have been made to synthesize it using different additives. In this way, titania and tialite have been added in different amounts to the initial raw material mixture (talc, kaolin, and synthetic alumina). In this research, the initial powders (talc, kaolin, and synthetic alumina) were mixed in a planetary ball mill using different amounts of TiO_2 and tialite. The mixtures were sintered at 1250, 1300, and 1350 °C for 3 h. X-ray diffractometry and fluorescence, thermal analysis, microstructural observation, density, and cold compressive strength (CCS) were used to evaluate the sintered samples. Phase analysis revealed the presence of the cordierite phase along with small amounts of spinel. With increasing sintering temperature and titania addition, the amount of spinel decreased and the amount of cordierite phase increased. The real density increased with increasing titania additive content, but at higher titania contents, microcracks were observed in the SEM micrographs. By adding 15 wt% of tialite to the initial batch, the compressive strength has been increased by 88% compared to the pure cordierite sample.

Keywords: Cordierite; Compressive strength; Synthesis; TiO_2;Tialite.

[DOI: 10.22068/ijmse.3659]

1. Introduction

Cordierite ceramic ($Mg_2Al_4Si_5O_{18}$) with its unique properties, such as low thermal expansion, high thermal shock resistance, low dielectric constant, and suitable refractoriness, has been widely used in various industrial applications [1,2]. This material is rarely found naturally, and its synthesis has been important since the past and has been used in various methods such as solid-state reaction, sol-gel method, co-precipitation, and solution combustion in academic and industrial fieldsand is under development [3–7].

Among these methods, the solid-state method has attracted the most attention from both industrialists and researchers due to its simplicity in the production process, which is a one-step process, its ability to use a wide range of raw materials, and its low cost and ease of use. In the solid-state synthesis of cordierite, SiO_2, Al_2O_3, MgO, or a combination of these oxides are generally used, which are present in raw materials or natural minerals. The use of natural minerals such as kaolin, talc, ball clay, feldspars, and dolomite in the synthesis of cordierite significantly reduces the production cost. On the other hand, the synthesis of this material is challenging due to the narrow sintering temperature range required to achieve high-purity cordierite [8–10]. In order to improve the sintering process, reduce the sintering temperature, and achieve the desired properties, several methods have been proposed, the most important of which is the use of sintering aids and additives. The effects of various additives, including bismuth oxide, boron oxide, phosphorus oxide, calcium oxide, magnesium oxide, yttria-stabilized zirconia, titanium oxide, and others, have been investigated by researchers to attain the desired properties of cordierite [11–16].

Considering the application of cordierite bodies as components in furnaces and catalyst supports in honeycomb structures, recently employed as a base for solar thermal energy storage and heat exchangers for gas turbine engines, among other applications subjected to continuous thermal, mechanical, and thermomechanical stresses, it is imperative to enhance the strength of these bodies. TiO_2 proves to be a suitable choice to improve the thermomechanical properties of cordierite bodies by adding it to the initial cordierite composition, aiming to reduce the sintering temperature and control the microstructure effectively [17–20].

[DOI: 10.22068/ijmse.3659]

The effect of adding different percentages of TiO_2 on the microstructure and properties of cordierite has been investigated in recent research, both below 3% and above 10% [16,21]. It is known that TiO_2 dissolves in the cordierite phase up to 3%, and higher amounts of it appear in the structure as different phases, such as tialite and $MgTi_2O_5$. In fact, with the presence of Al_2O_3 and TiO_2 in the composition, formation of a tialite phase becomes possible. This occurrence could potentially alter the stoichiometry of the composition and reduce the amount of cordierite phase.

Therefore, in this study, for the first time, 3, 6, and 9 wt% of TiO_2 additives were added to cordierite and compared with tialite additives with 5, 10, and 15 wt%. The tialite additive was synthesized separately using TiO_2 and Al_2O_3 raw materials at a temperature of 1300 °C. Notably, the cordierite was sintered utilizing natural raw materials of talc and kaolin and synthetic Al_2O_3 with accurate stoichiometric calculation by applying TiO_2 and tialite additives at different temperatures of 1250, 1300, and 1350 °C. Moreover, the effect of these additives and temperature was studied on the phase, microstructure, physical properties, and mechanical behavior.

2. Materials and Methods

2.1 Primary Materials

Talc ($Mg_3Si_4O_{10}(OH)_2$, 90% purity, < 40 μm, Iran), kaolin ($Al_2Si_2O_5(OH)_4$, 92% purity, <40 μm, Czech Republic), and alumina (γ-Al_2O_3, 99.95% purity, <20 μm, India) were chosen as the primary raw materials. Titanium dioxide with a purity of 99.95% and magnesium carbonate with a purity of 99.95% were also utilized as additives. The chemical composition of the mentioned raw materials is presented in Table 1. The designed formulas were based on the cordierite stoichiometry, with MgO: 13.7, Al_2O_3:34.9, and SiO_2: 51.4, by weight percent (Table 2). The sintered cordierite bodies at the temperatures of 1250, 1300, and 1350˚C are denoted by the abbreviations C-125, C-130, and C-135, respectively. The cordierite bodies with 3, 6, and 9 wt. % of TiO_2 are indicated by CT3, CT6, and CT9. Meanwhile, the cordierite bodies containing 5, 10, and 15 wt. % of tialite are specified by CAT5, CAT10, and CAT15, respectively. Also, the cordierite

[DOI: 10.22068/ijmse.3659]

bodies containing 5, 10, and 15 wt. % of tialite containing magnesia are indicated by CATM5, CATM10, and CATM15, respectively. A formulation was considered to achieve stoichiometric cordierite with 42.09% talc, 11.79% synthetic alumina, and 46.12% kaolin.

2.2. **Sample Preparation**

The raw materials were mixed in a planetary ball mill of zirconia cups and balls at a 5:1 ball-to-powder weight ratio. The mixture was rotated at 200 rpm for 1 h. Subsequently, the powder was mixed with a 5 wt. % PVA solution and allowed to age for 24 h. After aging, the mixture was passed through a 20-mesh sieve for further granulation. Using uniaxial pressing with a pressure of 14 bar, cylindrical samples with a diameter and height of 20 mm were formed. Green samples were dried in an oven at 100 °C for 24 h. Following drying, the samples were subjected to a controlled thermal cycle in a box electric furnace. The heating rate was set to 10 °C/min, with dwell times of 1 h at 500 °C and 30 min at 1000 °C. Finally, the samples were sintered at the temperatures of 1250, 1300, and 1350 °C for 3 h. The samples were allowed to cool naturally in the furnace to room temperature.

2.3. Characterization and Testing

Chemical analysis of the raw materials was conducted using an X-ray fluorescence spectrometer (PHILIPS PW1410, manufactured in the Netherlands). Thermal analysis (DTA-TG) of the initial powder mixture was performed using a device (STA 503-BHAR PL-STA 1460) with a heating rate of 10˚C/min in an argon atmosphere, considering the instrument's limitation up to 1200 degrees Celsius. Phase identification of synthetic powders and sintered ceramic bodies was determined by X-ray diffraction (Philips PW-3710) using Cu Kα radiation. The PANalytical XPert HighScore Plus software was utilized for qualitative analysis. After breaking the samples using an electric mortar, powders with particle sizes less than 45 μm were separated using a 325 mesh sieve for XRD analysis. Density and porosity of the samples were determined using the Archimedes method according to the ASTM C373 standard. The true density (powder) was measured using the AccuPyc 1330 v3.00 pycnometer. Relative density was calculated based on the

[DOI: 10.22068/ijmse.3659]

bulk density obtained from the Archimedes method. The microstructure and morphology of the sintered samples were examined using a scanning electron microscope (SEM) with a thin gold coating using the VEGA\TESCAN-XMU device. One of the methods for evaluating the mechanical properties of ceramic materials is the measurement of cold crushing strength (CCS). In this method, samples were subjected to pressure using a press, and the highest applied force immediately after fracture was recorded by a force sensor (load cell). The compressive strength was then calculated in megapascals.

3. Results and Discussion

3.1. TG-DTA

The thermal analysis of the raw materials of the two cordierite samples, one without additives (C) and another containing 9% titanium dioxide additive (CT9), was investigated according to Figure 1. In the synthesis of cordierite, two mineral substances, kaolin and talc, along with synthetic alumina, were used. In the thermal analysis of these materials, heat absorption and heat release peaks related to phase changes and moisture evaporation were observed. The thermal curve initially exhibited an endothermic peak between 110 and 215 degrees Celsius, attributed to the removal of absorbed water. Considering the sources of kaolin, talc, and magnesium carbonate, decomposition occurs at the mentioned temperatures. The occurrences for talc can be described as follows [22]:

$3MgO.\ 4SiO_2.\ H_2O$ (Talc) $\text{------}(350^0C\text{- }500^0C)\text{-----}\rightarrow 3MgO.\ 4SiO_2\ .\ (1\text{-}x)H_2O$

Nearly less than 1% of 7/4% of water (*OH*) is expelled from the talc structure.

$\text{-----}(600^0C\text{-}900^0C)\text{-----}\rightarrow 3MgOSiO_3$ (*Enstatite*) $+ SiO_2 + (1\text{-}x)H_2O$

The events for kaolinite present in kaolin, without considering stoichiometric coefficients, are as follows [22]:

$Al_2O_3\ .\ 2SiO_2\ .\ 2H_2O\ \text{-----}(450^0C)\text{-----}\rightarrow Al_2O_3\ .\ 2SiO_2\ {}_{+}\ 2H_2O$

[DOI: 10.22068/ijmse.3659]

-----(980^{0}C)-----→ $2Al_2O_3 . 3SiO_2$ (Al-Si Spinel) $_+$ SiO_2

-----(>1000^{0}C)-----→ $3Al_2O_3 . 2SiO_2$ (Mullite) $_+$ SiO_2

Considering the mentioned events, it can be stated that the two endothermic peaks observed around 500-600^{0}C are associated with the decomposition of kaolinite and the primary breakdown of talc. Both involve the release of OH groups from the structure, with the initial release occurring in talc and complete release later [18,23]. The endothermic peak around 900^{0}C corresponds to the decomposition of talc into enstatite and amorphous silica, accompanied by the residual hydroxyl groups (OH) as indicated by the weight loss in TG.

The exothermic peaks in the range of 900-1000^{0}C are related to the formation of Al-Si spinel phases with primary mullite from metakaolin. The possibility of spinel formation ($MgAl_2OH$) at temperatures above 1100^{0}C, characterized by a small exothermic peak, exists. There is also a likelihood of the formation of various magnesium titanates or aluminum titanate solid solutions containing magnesium ion substitution around 1200^{0}C, indicated by a very small endothermic peak and the absence of an exothermic peak. A small endothermic peak is observed in the DTA-TG curve of the CT9 sample at temperatures below 1200^{0}C (Figure 1b), possibly related to the formation of magnesium titanates or tialites containing magnesium ions [23,24].

Based on previous literature, with an increase in temperature in the DTA curve within the temperature range of 1200-1400^{0}C, one would expect to observe endothermic peaks indicating the phase transformation of mullite and spinel into cordierite [25]. However, due to the instrument's limitations up to 1200^{0}C, we were unable to identify these peaks.

3.2. Effect of TiO_2, Tialites, and Sintering Temperature on Phase Compositions

For further investigation of the temperature effect on the phase compositions of cordierite ceramics, samples sintered at temperatures of 1250, 1300, and 1350 degrees Celsius were collected through XRD analysis, as

[DOI: 10.22068/ijmse.3659]

shown in Figure 2. According to Figure 2a, the primary crystalline phase, cordierite, with reference code (01-084-1220), and the secondary spinel phase Mg-Al, with reference code (96-900-3488), were observed.

As illustrated in the X-ray diffraction patterns in Figure 2a, the formation of cordierite occurred effectively at 1250^0C, accompanied by spinel. To enhance the amount of cordierite and improve their crystallographic order, higher temperatures were also employed. Additionally, the possibility of partial melt phase formation resulting from impurities may contribute to the dissolution of other partial phases and facilitate the easier penetration of Mg^{2+}, Al^{3+}, and Si^{4+} ions, resulting in increased cordierite content [26].

In the synthesis of the base formula of synthetic cordierite (a mixture of talc, kaolin, and alumina), varying amounts of TiO_2 (three, six, and nine weight percent) were added. After mixing and preparing cylindrical samples, they were sintered at temperatures of 1250°C, 1300°C, and 1350°C for three h. Subsequently, X-ray diffraction patterns of the samples, such as CT3 containing different TiO_2 percentages at various sintering temperatures, were obtained, as depicted in Figure 2b.

As observed, the primary phases in all 3% TiO_2-containing samples sintered at different temperatures were cordierite and spinel ($MgAl_2O_4$). With an increase in the percentage of TiO_2, phases such as $MgTiO_5$ and $AlTiO_5$ were identified in samples CT3, CT6, and CT9. It is noted that the cordierite content increased with increasing temperatures. The formation of new alpha-cordierite may be due to the transformation of remaining materials, including mullite (from kaolin) and enstatite (from talc), along with alumina. Since the percentage of these remaining materials is less than 3% by weight, their peaks were not observed in the X-ray diffraction pattern.

According to the literature, TiO_2 partially dissolves in mullite, spinel, and cordierite, and if it exceeds a certain limit, it can contribute to separate phases such as tialite. Mullite can dissolve a maximum of 4% by weight TiO_2 and 12.5% Fe_2O_3 [27]. The addition of TiO_2 reduces the likelihood of alumina presence, favoring increased mullite content [28]. TiO_2 can dissolve in spinel ($MgAl_2O_4$) up to about 2% by weight,

[DOI: 10.22068/ijmse.3659]

beyond which various phases containing TiO_2, such as $MgTiO_5$, Mg_2TiO_4, tialite containing magnesium ($MgxAl_{2(1-x)}Ti_{(1-x)}O5$), etc., may form [29].

The addition of TiO_2 to a cordierite-based material reduces the sintering temperature and generally has a positive effect on cordierite crystallization, and the liquid phase created during sintering can typically act as a germinating agent. TiO_2 can dissolve up to about 3% by weight in the cordierite composition; beyond that, it may present itself as separate phases. Moreover, TiO_2 delays the spinel formation during cordierite formation, leading to an increase in cordierite content [4,22].

According to the study by Luo and colleagues [21], in TiO_2-containing cordierite, the possibility of forming different phases in terms of free energy was investigated. The likelihood of forming cordierite is higher than other phases, while the probability of forming tialite is the lowest. The likelihood of forming phases such as $MgTiO_3$, $MgTi_2O_5$, and $MgTi_2O_4$, which have higher coefficients of expansion than tialite, is higher. As per the XRD results in our research, the $MgTi_2O_5$ phase has been identified, consistent with Figure 2.

To address the substantial differences in thermal expansion coefficients between the phases remaining after the addition of TiO_2, such as TiO_2 itself and cordierite, and considering that part of the added TiO_2, along with alumina, transforms into tialite, potentially leading to an insufficient alumina content for cordierite formation, the decision was made to independently synthesize tialite and subsequently introduce it into the mixture of kaolin, talc, and alumina. In this context, the tialite phase was initially synthesized from a combination of titanium dioxide and alumina, adhering to a stoichiometric ratio derived from recent research.

Recognizing that tialite is a semi-stable phase below 1280°C, measures were taken to prevent its decomposition. MgO was added to stabilize tialite. The X-ray diffraction pattern of the tialite-containing magnesia sample is depicted in Figure 3a. The required MgO content was set at 4% by weight, and the temperature for both tialite preparation and tialite-containing magnesia synthesis was maintained at 1350°C for a duration of 8 h [22,30].

[DOI: 10.22068/ijmse.3659]

As evident in Figures 3a and 3b, all samples exhibit the primary alpha-cordierite phase, accompanied by spinel and tialite phases. Researchers have explored the synthesis of cordierite composites with tialite using the sol-gel method. Their findings reveal the presence of cordierite, tialite, and traces of rutile and mullite at 1200°C, with the notation that tialite slightly reduces the crystallization of cordierite [31].

3.3. Effect of TiO_2, tialite, and sintering temperature on microstructures

The investigation of the microstructure of the samples utilized a scanning electron microscope (SEM). In Figure 4, micrographs "a" and "b" correspond to the microstructure of sample C-125 (the pure cordierite sample was sintered at 1250°C) at the magnifications of 500 and 1000 times, respectively. Additionally, Figures 4 "c" and "d" depict micrographs at 500 and 1000 times magnification for sample C-135 (the pure cordierite sample was sintered at 1350°C). Examining the micrographs reveals the presence of the cordierite matrix phase alongside intermediate phases. With the increase in firing temperature, some of these intermediate phases have transformed into cordierite, corroborated by XRD analysis in Figure 2.

Comparing micrographs "a" and "c," a noticeable reduction in porosity is observed with the increase in sintering temperature from 1250 to 1350°C. This phenomenon can be attributed to the enhanced sinterability of the sample at higher temperatures, as supported by the XRD analysis in Figure 2.

Further analysis of samples C-125 and C-135 at a magnification of 7000 times, along with energy-dispersive X-ray spectroscopy (EDS) analysis, reveals that the grayish background corresponds to the cordierite phase. It appears that in addition to cordierite, a mixture of cordierite and spinel ($MgAl_2O_4$) and possibly some mullite may be present, although their identification is challenging due to their low content in X-ray diffraction.

Exploring the effects of titanium dioxide additive on the microstructure of sample CATM15, SEM micrographs in Figure 5 (a, b) at magnifications of 500 and 1000 reveal the gray areas corresponding to the cordierite matrix phase, black regions representing structural porosity, bright gray points likely associated with intermediate phases such as spinel and mullite, and a mixture of intermediate phases and cordierite

[DOI: 10.22068/ijmse.3659]

that hasn't completely transformed. The bright spots are attributed to phases containing titanium, as confirmed by EDS analysis in Figure 5c. The presence of titanium additive, replacing Ti^{4+} with Al^{3+}, increases the available vacant space in the structure for ion penetration, enhancing the likelihood of completing the phase transition to cordierite. Consequently, intermediate phases like spinel and mullite are less pronounced compared to samples without additives, as observed in the X-ray diffraction phase analysis, aligning with the intensity reduction of spinel and mullite peaks. This observation is consistent with Figure 2, demonstrating a correlation with XRD phase analysis. Furthermore, the comparison of these microstructures with other studies suggests the possible presence of an amorphous phase in the samples [16,21].

3.4. Investigation of density and porosity of cordierite samples containing titanium dioxide additives

The samples include pure cordierite (C) and cordierite with 3%, 6%, and 9% TiO_2 additives (CT3, CT6, CT9), heat-treated at 1250°C, 1300°C, and 1350°C. True and bulk densities, along with open porosity, were measured using pycnometry and Archimedean methods (Figure 6). The true density of the specimens ranged from 2.53 to 2.62 g/cm³. As shown in Figure 6b, CT6 and CT9 exhibited the highest true densities, while C and CT3 had similar values. True density variations of 0.01–0.03 g/cm³ can be attributed to experimental errors and depend on the density and proportions of individual phases. Theoretical densities of relevant phases include: cordierite (2.57–2.66 g/cm³), spinel (3.58 g/cm³), mullite (3.2 g/cm³), rutile (4.25 g/cm³), tialite (3.7 g/cm³), $MgTi_2O_5$ (3.48 g/cm³), amorphous phase (2.2–2.4 g/cm³), and corundum (3.99 g/cm³). Despite the expectation that increasing temperatures would lead to notable alterations in actual density due to variations in the amount of phases present, such changes were not observed.

Based on the bulk density results (Figure 6a), an increase in sintering temperature from 1250°C to 1350°C slightly decreases bulk density by approximately 0.08 g/cm³, with CT9-125 displaying the highest value (2.18 g/cm³). Although bulk density is typically increased as a result of an elevation in temperature, phase transformations at higher temperatures have resulted in microcracks, reducing bulk density. Similar

[DOI: 10.22068/ijmse.3659]

observations by Marikana et al. [16] attribute this reduction to the formation of a quartz phase and subsequent cracking due to volumetric expansion at high temperatures.

Relative density trends (Figure 6d) indicate that CT3 at 1250°C achieves the highest relative density (84.5%), while samples at 1350°C exhibit the lowest (80–83.5%). Porosity trends (Figure 6c) confirm that minimal porosity (~8%) occurs at 1350°C for pure cordierite. However, porosity increases for all samples at 1350°C due to microcracks caused by phase transformations, such as spinel and mullite transitions to cordierite, partial tialite decomposition, quartz transformations, and thermal expansion mismatches.

Marikana et al. [16] reported that incorporating 10–20 wt% TiO_2 into cordierite increases the thermal expansion coefficients by as much as 80% owing to the development of other phases, excluding tialite, which possesses a low thermal expansion coefficient. Therefore, sintering temperatures of 1250–1300°C are optimal for pure cordierite and TiO_2-containing compositions, minimizing porosity and avoiding detrimental microcrack formation.

3.5. Density and Porosity Investigation of Cordierite Samples Containing Tialite Additive

Tialite was added to cordierite raw materials in amounts of 5, 10, and 15 wt% and sintered at 1300°C. Separately, tialite was synthesized at 1300°C with (CATM) and without (CAT) magnesium carbonate, then introduced as an additive. Pycnometric analysis (Figure 7) showed that real density increased with higher tialite content, consistent with the mixture rule, due to tialite's higher density.

Figure 7 also indicates that CATM samples exhibit better relative density compared to CAT samples, with a more stable trend. The absence of magnesia in CAT samples increases the likelihood of tialite decomposition into Al_2O_3 and TiO_2. Decomposition may initiate below 1280°C, hindering the sintering process. Overall, increasing the content of tialite or magnesia-stabilized tialite enhances refractoriness but reduces sintering.

3.6. Investigation of the Compressive Strength of Different Cordierite Samples Containing Titanium Dioxide and Tialite Additives

[DOI: 10.22068/ijmse.3659]

The mechanical behavior of cordierite samples at sintering temperatures of 1250-1300-1350 degrees Celsius and with the influence of various percentages of titanium dioxide (TiO_2) and tialite additives was examined. In Figure 8a, the compressive strength of cordierite-titanium dioxide samples is observed. The pure cordierite sample exhibited compressive strength in the range of 124-139 MPa, reaching the highest strength at a sintering temperature of 1350 degrees Celsius. The compressive strength results of cordierite samples with different percentages of TiO_2 after sintering at temperatures from 1250 to 1350 degrees Celsius are shown in Figure 8.

As evident in the figure, the highest strengths belong to samples containing six percent TiO_2, ranging from 156 to 176 MPa. X-ray diffraction patterns indicate the presence of cordierite, spinel, mullite, $MgTi_2O_5$, tialite, and possibly an amorphous phase in TiO_2-containing samples (Figures 2 and 3).

As mentioned earlier, part of the added TiO_2 dissolves in the cordierite phase, contributing to increased strength. It also contributes to the formation of spinel, mullite, $MgTi_2O_5$, tialite, and amorphous phases, with some portions remaining. In general, the formation of spinel and mullite, along with the presence of residual TiO_2, delays the cordierite system's refractoriness, making sintering harder to implement. The formation of an amorphous phase containing TiO_2 can also contribute to increased sintering. Therefore, four simultaneous phenomena occur, and achieving desirable results requires controlling the microstructure. It appears that we have not succeeded in controlling the conditions for CT3 and CT9 in this project. The four phenomena are as follows:

A) Dissolution of TiO_2 in cordierite, elevation of sinterability, and formation of more cordierite;

B) Formation of high-melting-point phases such as spinel and $MgTi_2O_5$ relative to cordierite;

C) Changes in the type and amount of the amorphous phase in the presence of TiO_2; and

D) Existence of various stresses at grain boundaries due to the presence of phases with different thermal expansion coefficients.

[DOI: 10.22068/ijmse.3659]

The compressive strength of cordierite-tialite and cordierite-tialite samples containing magnesia additive is presented in Figure 8b. The samples were sintered at a constant temperature of 1300 degrees Celsius. As observed, the compressive strength of cordierite-tialite samples with 10 and 15 weight percent tialite additives has significantly increased. It is much higher than the samples without additives, reaching approximately 240 MPa in the CAT15 sample, indicating nearly a twofold increase compared to the cordierite sample without additives.

It appears that due to the better match of the thermal expansion of tialite and cordierite in these samples, residual stress at grain boundaries during sintering is very low. This results in the composite demonstrating greater resistance when subjected to external stress. On the other hand, the presence of the tialite phase in the body contributes to the increased toughness of the cordierite body. In a study, it was mentioned that the toughness of cordierite bodies with 10% TiO_2 sintered at 1300 degrees Celsius, where tialite, rutile, and cristobalite, along with the main cordierite phase, are present, is around 3.28 $MPa.m^{1.2}$, compared to the denser cordierite body of 2.87 $MPa.m^{1.2}$ [30]. This phenomenon is more pronounced in bodies containing tialite because the formation of unwanted phases is prevented.

In cordierite-tialite samples containing magnesia (CATM), there is almost no significant change in compressive strength with the increase in tialite additive percentage compared to the cordierite sample. This is because these phenomena are in conflict with each other in these samples, with some improving strength and others reducing it, and their overall effect is balanced.

a) ATM, represented by the formula Al_{2-2x} Mgx Ti_{1+x} O_5, exhibits greater stability compared to tialite (AT) Al_2TiO_5 at temperatures below 1280 degrees Celsius. Consequently, the likelihood of its decomposition is lower. During decomposition, ATM undergoes transformation into TiO_2, Al_2O_3, and $MgAl_2O_4$ spinel, while tialite (AT) transforms into TiO_2 and Al_2O_3. Overall, due to the reduced probability of decomposition, its role in mitigating stress at the interfaces of the cordierite-ATM sample (CATM) appears to be less pronounced.

[DOI: 10.22068/ijmse.3659]

b) ATM possesses a higher coefficient of thermal expansion compared to AT. This results in increased stress between the grains of cordierite and ATM, as opposed to cordierite and AT, potentially leading to a decrease in strength.

It appears that in cordierite-ATM samples, the combined effect of these two properties contributes to the preservation of their compressive strength.

4. Conclusion

By using talc, kaolin, and synthetic alumina, a cordierite body with relatively high purity was synthesized at different temperatures. Titanium dioxide (TiO_2) and tialite were incorporated into the initial composition. The phase analysis, microstructure examination, physical properties, and mechanical behavior of the samples were evaluated. Key observations include:

1. Cordierite formation at 1250 degrees Celsius, accompanied by a small amount of Al-Mg spinel, occurred effectively. According to XRD results, increasing the sintering temperature to 1300 and 1350 degrees Celsius facilitated the easier penetration of Mg^{2+}, Al^{3+}, and Si^{4+} ions, resulting in a higher content of cordierite.

2. The presence of spinel in the XRD results indicates that the reaction of Mg-Al spinel with SiO2 to form cordierite requires a higher temperature. Adding TiO_2 tends to form phases with lower melting points; therefore, the formation of the cordierite phase increased.

3. With an increase in the sintering temperature and the percentage of TiO_2 additive, the real density of the samples increased. However, due to the formation of microcracks in the structure with an increase in the TiO_2 percentage, the bulk density decreased. Nevertheless, the highest relative density was obtained for CT3 at a sintering temperature of 1250 degrees Celsius with a percentage of 84.5%.

4. At the synthesis temperature of 1300 degrees Celsius, the compressive strength of sample CT6-130 increased by 30%, reaching 176.2 ± 9.4 MPa compared to pure cordierite (C-130).

[DOI: 10.22068/ijmse.3659]

5. The addition of 15% tialite to the initial cordierite mixture (sample CAT15-130) resulted in an 88% increase in compressive strength, reaching 239.9 ± 10.1 MPa compared to C-130. However, in samples containing tialite with magnesium additive (CATM), no significant changes in compressive strength were observed, remaining constant relative to the pure sample.

Acknowledgement

This research work has been supported with research grant (No.: 380682) by Materials and Energy Research Center (MERC), Karaj, Iran.

References

[1] Chowdhury, A., Maitra, S., Das, H.S., Sen, A., Samanta, G.K. and Datta, P., "Synthesis, properties and applications of cordierite ceramics, part 2" InterCeram Int. Ceram. Rev., 2007, 56, 98-102.

[2] Li, Y., Wang, J., Sun, L. and Wang, J., "Mechanisms of ultralow and anisotropic thermal expansion in cordierite Mg2Al4Si5O18: Insight from phonon behaviors" J. Am. Ceram. Soc., 2018, 101, 4708-4718.

[3] Ianoş, R., Lazău, I. and Păcurariu, C., "Solution combustion synthesis of α-cordierite" J. Alloys Compd., 2009, 480, 702-705.

[4] Tabit, K., Waqif, M. and Saâdi, L., "Crystallization behavior and properties of cordierite synthesized by sol-gel technique and hydrothermal treatment" J. Aust. Ceram. Soc., 2019, 55, 469-477.

[5] Lin, Y.H., Yen, F.S., Hsiang, H.I. and Lee, M.N., "Quasi-synchronous solid-state reaction for cordierite powder synthesis" Int. J. Appl. Ceram. Technol., 2024, 21, 169-182.

[6] Radev, L., Samuneva, B., Mihailova, I., Pavlova, L. and Kashchieva, E., "Sol-gel synthesis and structure of cordierite/tialite glass-ceramics" Process. Appl. Ceram., 2009, 3, 125-130.

[7] Hirano, M. and Inada, H., "Preparation and characterization of cordierite-zirconia composites from

[DOI: 10.22068/ijmse.3659]

co-precipitated powder" J. Mater. Sci., 1993, 28, 74-78.

[8] Phuc, N.H.H., Okuno, T., Matsuda, A. and Muto, H., "Ex situ Raman mapping study of mechanism of cordierite formation from stoichiometric oxide precursors" J. Eur. Ceram. Soc., 2014, 34, 1009-1015.

[9] Gibbs, G. V., "The polymorphism of cordierite. I. The crystal structure of low cordierite" Am. Miner., 1966, 51, 1068-1087.

[10] Eftekhari-Yekta, B., Ebadzadeh, T. and Ameri-Mahabad, N., "Preparation of porous cordierite bodies for use in catalytic converters" Adv. Appl. Ceram., 2007, 106, 276–280.

[11] Malachevsky, M.T., Fiscina, J.E. and Esparza, D.A., "Preparation of Synthetic Cordierite by Solid-State Reaction via Bismuth Oxide Flux" J. Am. Ceram. Soc., 2001, 84, 1575-1577.

[12] Redaoui, D., Sahnoune, F. and Heraiz, M., "Effect of B_2O_3 on phase transformation of cordierite synthesized from algerian kaolin and MgO" Acta Phys. Pol. A, 2018, 134, 75--78.

[13] Luo, L., Zhou, H. and Xu, C., "Microstructural development on sol-gel derived cordierite ceramics doped B_2O_3 and P_2O_5" Mater. Sci. Eng. B, 2003, 99, 348-351.

[14] Torres, F.J. and Alarcón, J., "Effect of MgO/CaO ratio on the microstructure of cordierite-based glass-ceramic glazes for floor tiles" Ceram. Int., 2005, 31, 683-690.

[15] Wang, L., Ma, B., Ren, X., Yu, C., Tian, J., Liu, C., Deng, C., Hu, C., Liu, Z., Yu, J. and Jiang, Z., "Phase-engineering strategy of ZrO_2 for enhancing the mechanical properties of porous cordierite ceramics", Mater. Today Commun., 2022, 30, 103032.

[16] Marikkannan, S.K. and Ayyasamy, E.P., "Synthesis, characterisation and sintering behaviour influencing the mechanical, thermal and physical properties of cordierite-doped TiO_2" J. Mater. Res. Technol., 2013, 2, 269–275.

[DOI: 10.22068/ijmse.3659]

[17] Lao, X., Xu, X., Jiang, W., Liang, J., Miao, L. and Wu, Q., "Influences of impurities and mineralogical structure of different kaolin minerals on thermal properties of cordierite ceramics for high-temperature thermal storage" Appl. Clay Sci., 2020, 187, 105485.

[18] Weaver, D.T., Van Aken, D.C. and Smith, J.D., "The role of TiO_2 and composition in the devitrification of near-stoichiometric cordierite" J. Mater. Sci., 2004, 39, 51-59.

[19] Dorado, B., Moreno-Sanabria, L., García, E., Belmonte, M., Miranzo, P. and Osendi, M.I., "3D printing of cordierite materials from raw reactive mixtures", Ceram. Int., 2023, 49, 4578-4585.

[20] Boldizsár, T., Bali, H., Szenti, I., Sebők-Papp, I., Bán, Z., Herczeg, S., Barna, G., Sápi, A., Kukovecz, A. and Kónya, Z., "Environmental-friendly economical cordierite-mullite-based ceramics for kiln furniture production and supports for CO_2 hydrogenation towards C5+ fuels" J. Eur. Ceram. Soc., 2023, 43, 5596-5605.

[21] Luo, X., Qu, D., Zhang, G. and Liu, H., "The influence of TiO_2 on synthesizing the structure of the cordierite" Adv. Mater. Res., 2011., 233-235, 3027-3031.

[22] Wu, J., Hu, C., Xu, X., Zhang, Y., Lu, C. and Wang, D., "Preparation and thermal shock resistance of cordierite-spodumene composite ceramics for solar heat transmission pipeline" Ceram. Int., 2016, 42, 13547–13554.

[23] Farzalipour Tabriz, M. and Ghassemi Kakroudi, M., " Thermo-mechanical design optimization of cordierite-mullite based kiln furniture" Iran. J. Mater. Sci. Eng., 2010, 7, 35-41.

[24] Ford, W.F., "The effect of heat on ceramics" Maclaren, 1967.

[25] Hamanaka, T., "Extruded Cordierite Honeycomb Ceramics for Environmental Applications" Handb. Adv. Ceram. Mater. Appl. Process. Prop., 2003, II, 367-384.

[26] Wang, J., Peng, Z., Chen, Y., Bao, W., Chang, L. and Feng, G., "In-situ hydrothermal synthesis of Cu-SSZ-13/cordierite for the catalytic removal of NO_x from diesel vehicles by NH_3" Chem. Eng. J.,

[DOI: 10.22068/ijmse.3659]

2015, 263, 9-19.

[27] Yalamaç, E. and Akkurt, S., "Additive and intensive grinding effects on the synthesis of cordierite", Ceram. Int., 2006, 32, 825–832.

[28] Stein, A., Keller, S.W. and Mallouk, T.E., "Turning down the heat: Design and mechanism in solid-state synthesis", Science, 1993, 80, 259, 1558-1564.

[29] Banjuraizah, J., Mohamad, H. and Ahmad, Z.A., "Crystal structure of single phase and low sintering temperature of α-cordierite synthesized from talc and kaolin" J. Alloys Compd., 2009, 482, 429-436.

[30] Ogiwara, T., Noda, Y. and Kimura, O., "Fabrication of high density cordierite ceramics using a coal fly ash" J. Ceram. Soc. Japan., 2010, 118, 231-235.

[31] Valášková, M., "Clays, clay minerals and cordierite ceramics - A review", Ceram. - Silikaty., 2015, 59, 331-340.

[DOI: 10.22068/ijmse.3659]

Table 1. XRF analysis of primary materials (Wt%)

Sample	Alumina	Titania	Magnesium carbonate	Talc	Kaolin
SiO_2	N	N	4.02	51.54	44.29
Al_2O_3	99.01	3.04	0.24	2.34	38.78
Fe_2O_3	N	N	0.10	1.47	1.33
CaO	0.07	0.08	8.58	1.44	0.19
MgO	N	N	39.86	26.32	0.25
Na_2O	0.18	0.05	0.20	0.57	0.13
K_2O	N	N	0.07	0.02	0.66
TiO_2	0.03	95.16	0.06	0.11	0.37
MnO	0.01	0.01	0.01	0.03	0.02
P_2O_5	0.00	0.02	0.01	0.07	0.07
LOI	0.37	1.37	46.70	15.29	12.97

[DOI: 10.22068/ijmse.3659]

Table 2. Information related to coding samples including sintering temperature, and additive

Code	Sintering Temperature (^{0}C)	Additive amount	Additive
C-125	1250	0	No additive
C-130	1300		
C-135	1350		
CT3-125	1250	3	Titania
CT3-130	1300		
CT3-135	1350		
CT6-125	1250	6	
CT6-130	1300		
CT6-135	1350		
CT9-125	1250	9	
CT9-130	1300		
CT9-135	1350		
CAT5-130	1300	5	Tialite
CAT10-130	1300	10	
CAT15-130	1300	15	
CATM5-130	1300	5	Tialite containing magnesium oxide
CATM10-130	1300	10	
CATM15-130	1300	15	

[DOI: 10.22068/ijmse.3659]

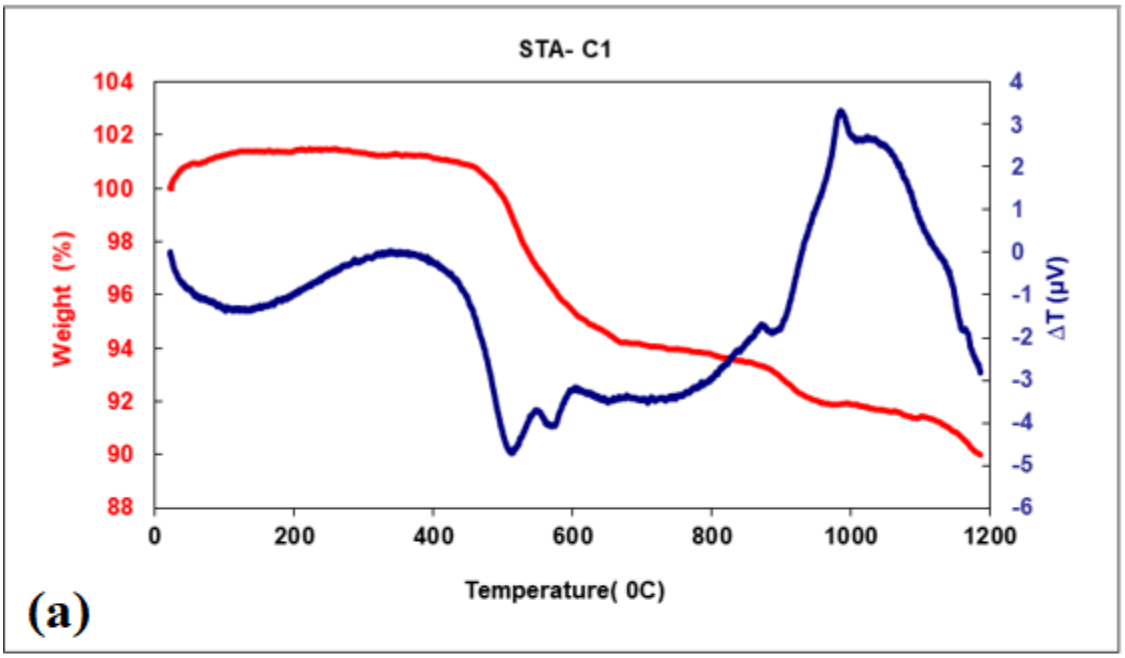

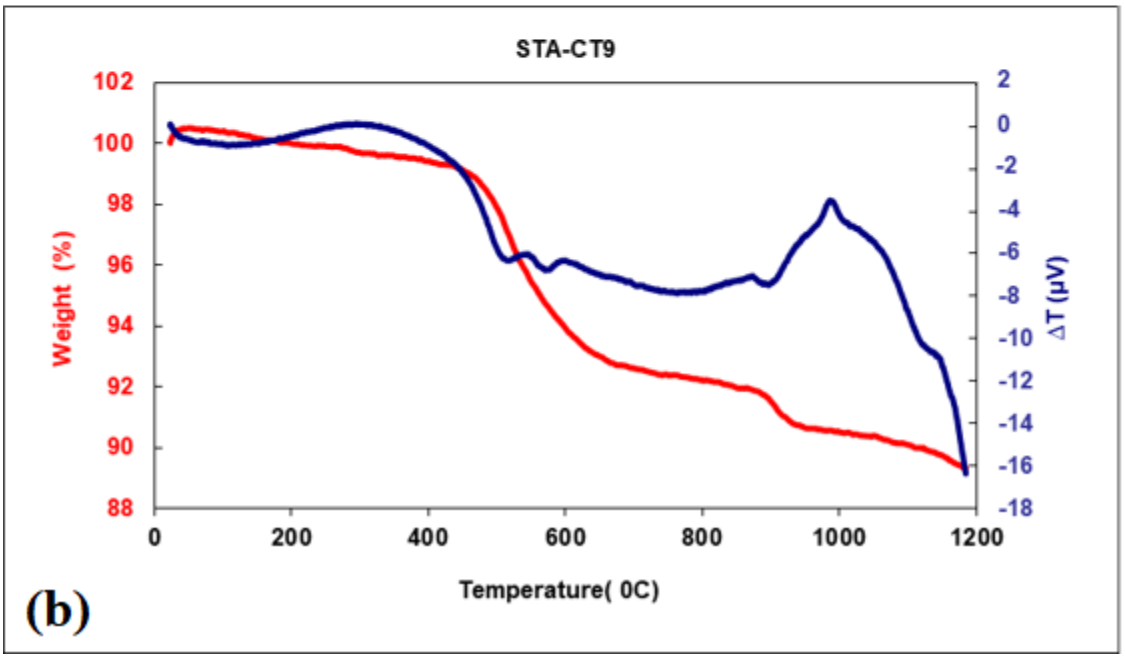

Figure 1: DTA-TG diagram of samples (a) Pure Cordierite and (b) Cordierite containing 9% Titanium Dioxide Additive

[DOI: 10.22068/ijmse.3659]

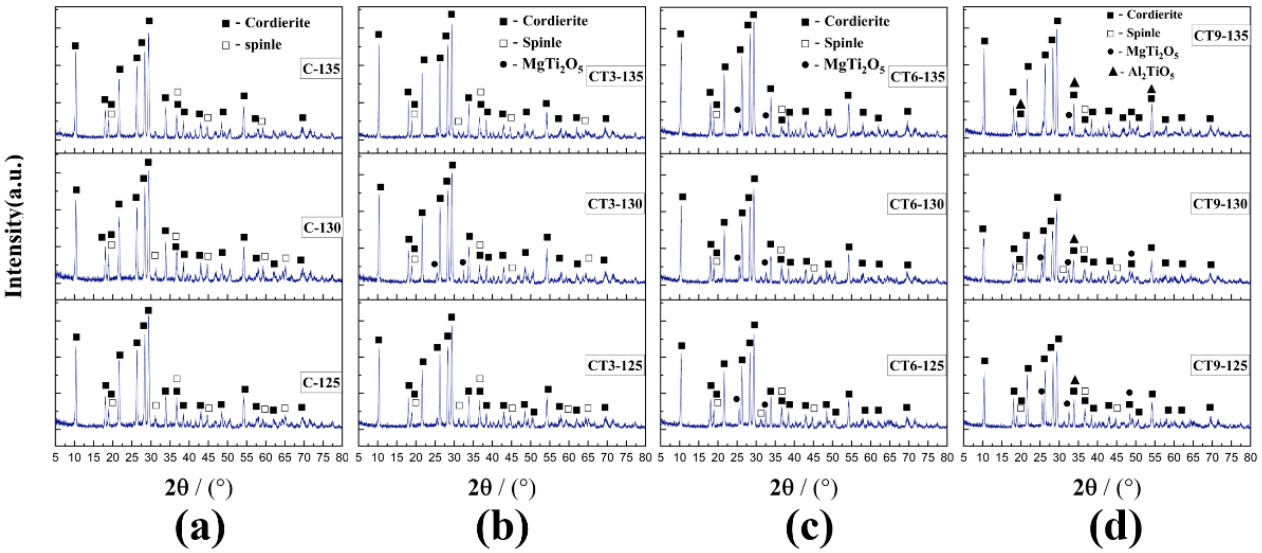

Figure 2: XRD analysis of cordierite samples at different temperatures (1250°C, 1300°C, and 1350°C): (a) Cordierite (C-125, C-130, and C135), (b) Cordierite with 3 wt. % of TiO_2 (CT3-125, CT3-130, and C T3-135), (c) Cordierite with 6 wt. % of TiO_2 (CT6-125, CT6-130, and C T6-135), and (d) Cordierite with 9 wt. % of TiO_2 (CT9-125, CT9-130, and C T9-135)

[DOI: 10.22068/ijmse.3659]

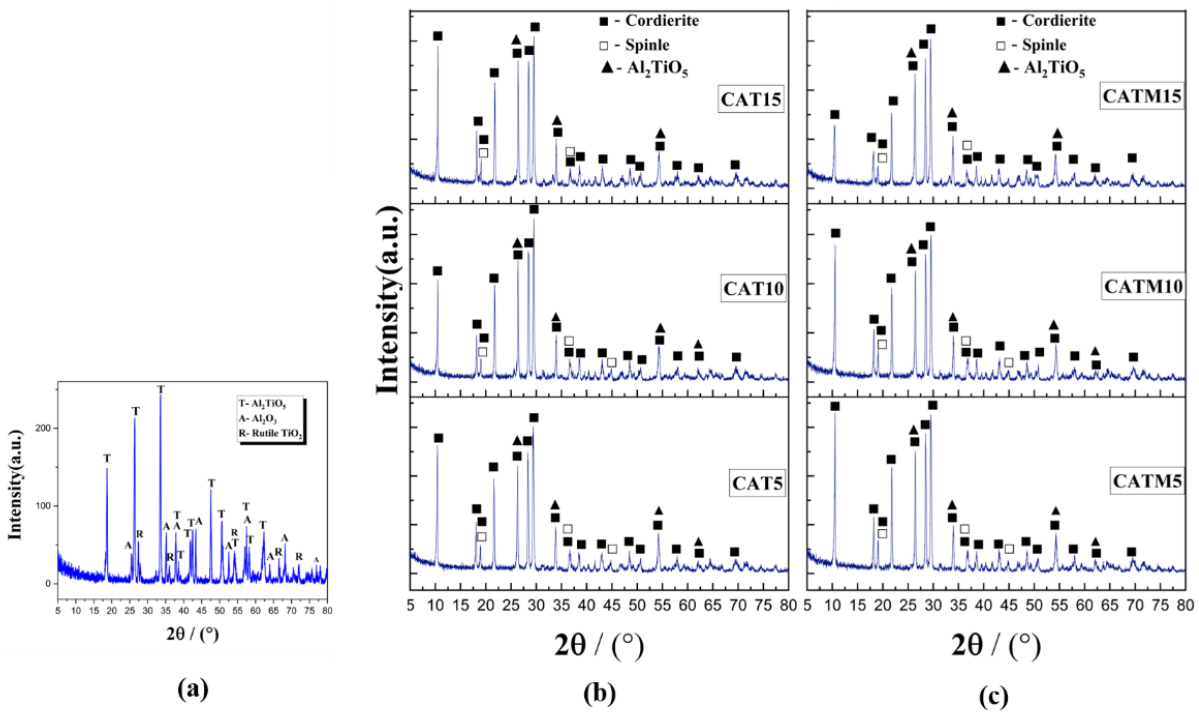

Figure 3: XRD analysis of the synthesized samples: (a) Tialite with 4 wt. % of magnesia, (b) Cordierite containing 5, 10, and 15 wt. % of tialite (CAT5, CAT10, and CAT15), and (c) Cordierite containing 5, 10, and 15 wt. % of tialite containing magnesia (CATM5, CATM10, and CATM15)

[DOI: 10.22068/ijmse.3659]

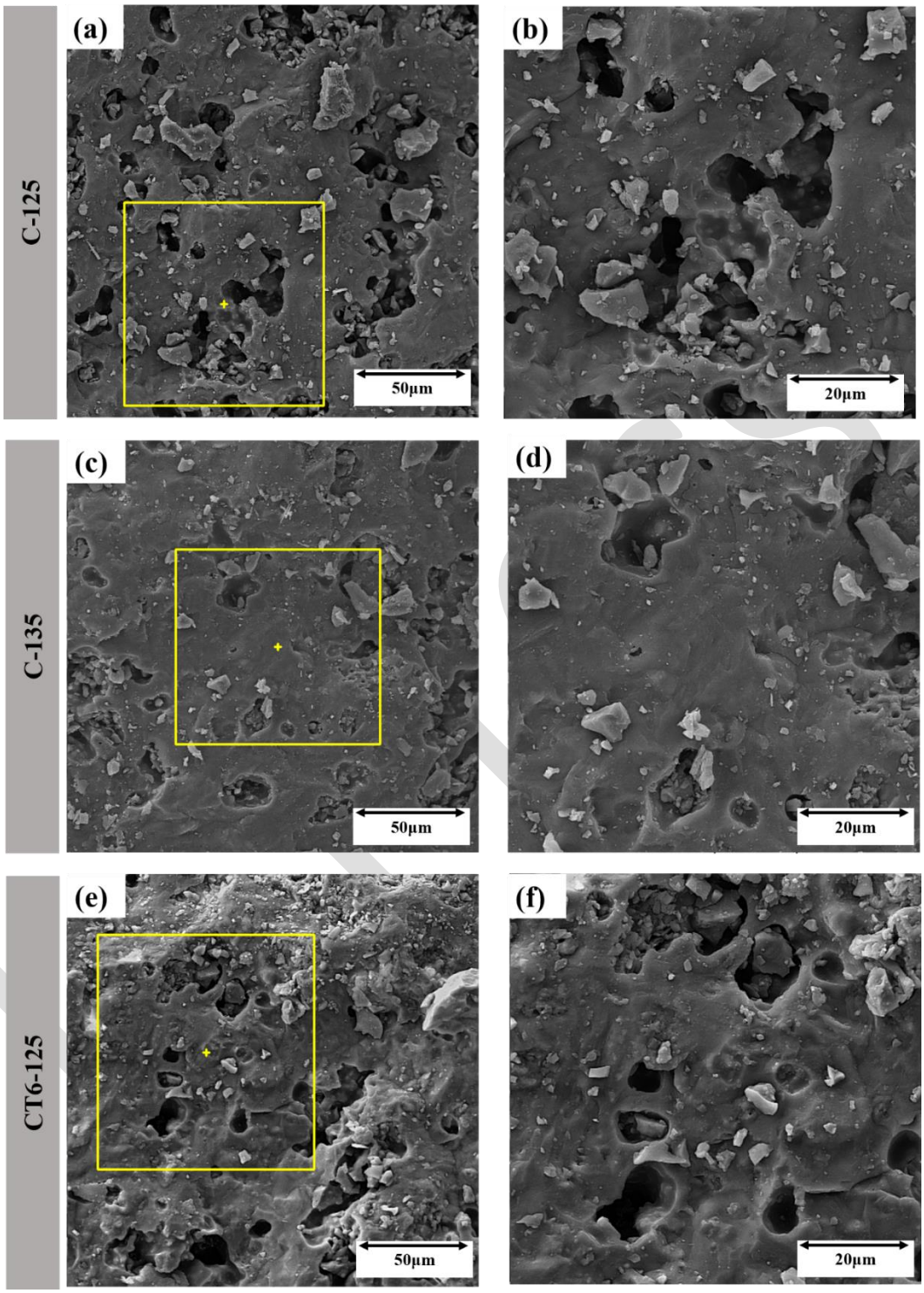

Figure 4: SEM micrographs of the fractured surface of C-125 (a, b), C-135 (c, d), and CT6-125 (e, f) samples at magnifications of 500 and 1000 times, respectively.

[DOI: 10.22068/ijmse.3659]

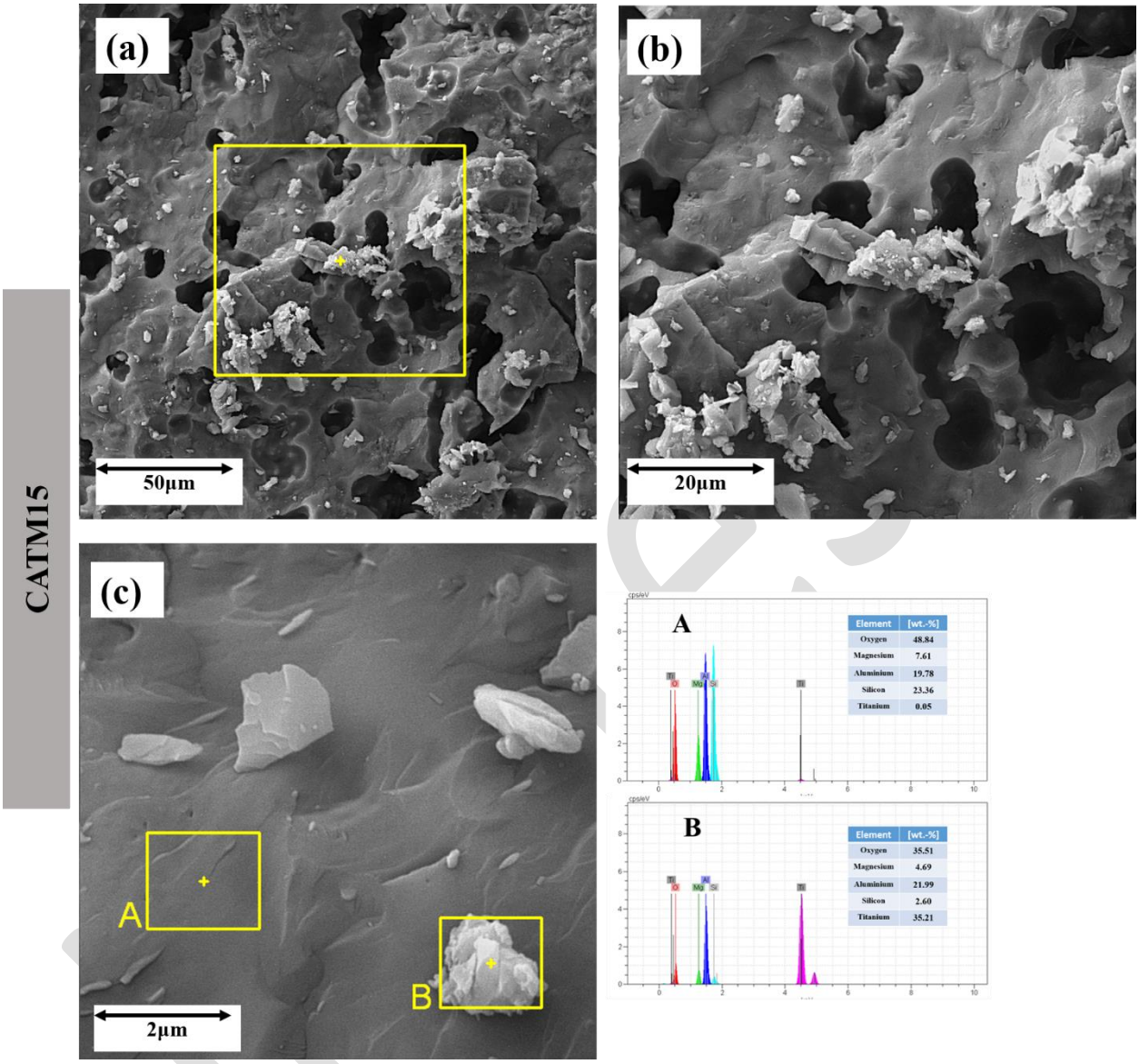

Figure 5: SEM micrographs of the fractured surface of CATM15 sample at different magnifications (a) 500x, (b) 1000x, and (c) 7000x, along with elemental analysis

[DOI: 10.22068/ijmse.3659]

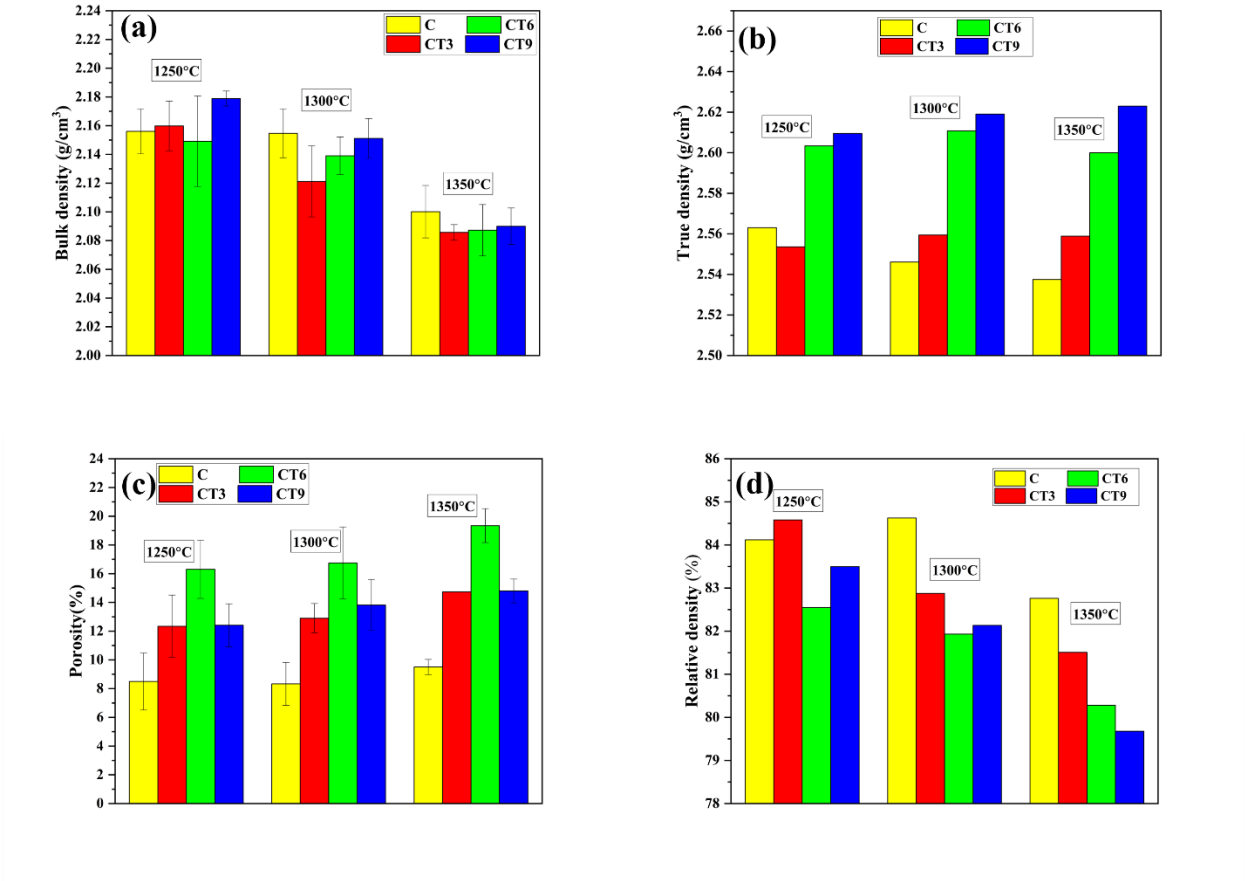

Figure 6: Comparison of (a) bulk density, (b) true density, (c) percentage of porosity, and (d) relative density of pure cordierite and cordierite containing TiO_2 additive after sintering at different temperatures.

[DOI: 10.22068/ijmse.3659]

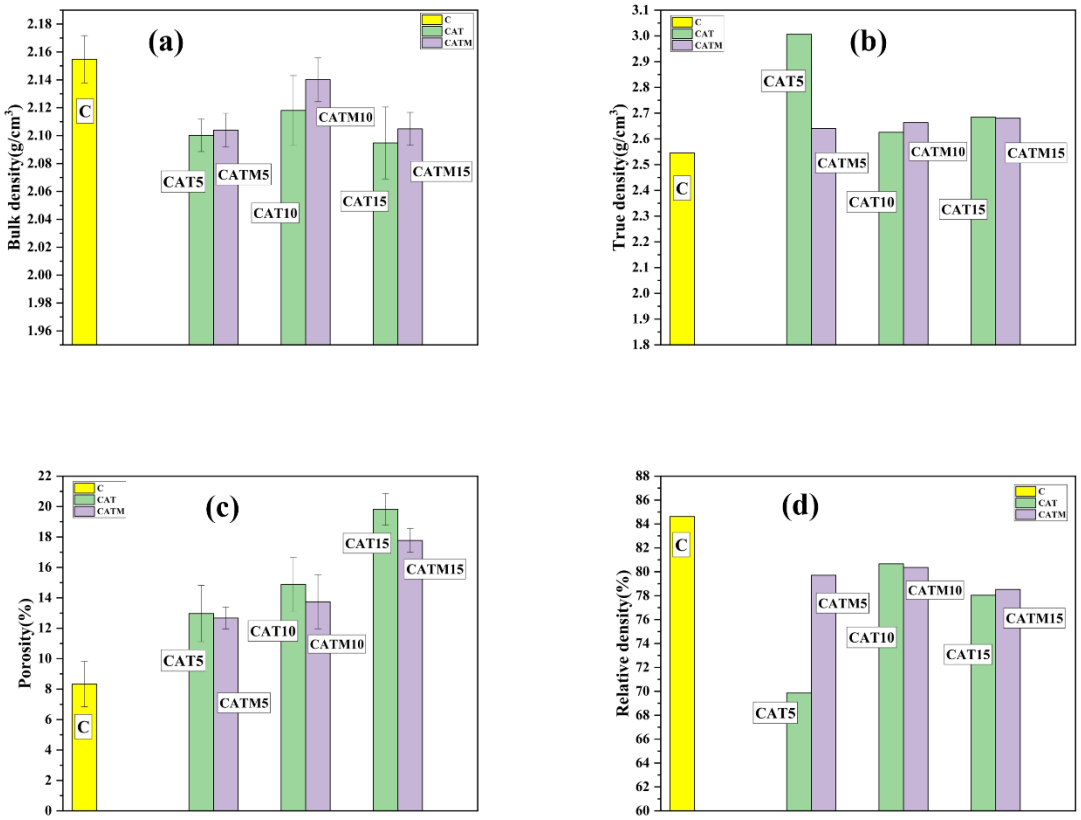

Figure 7: Comparison of (a) Bulk Density, (b) Real Density, (c) Percentage of Porosity, and (d) Relative Density of Pure Cordierite-Tialite and Cordierite-Tialite Samples with Magnesia Additive after Sintering at 1300 degrees Celsius

[DOI: 10.22068/ijmse.3659]

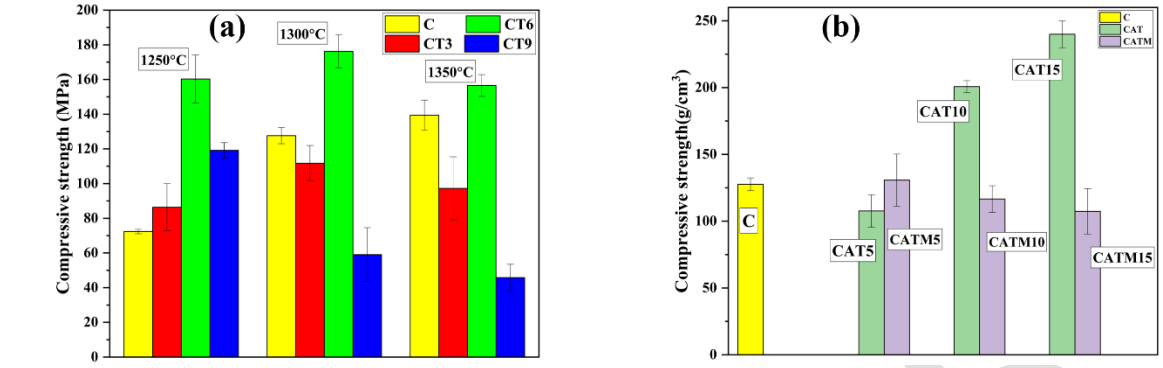

Figure 8: the comparison of compressive strength for pure cordierite samples with (a) cordierite containing TiO_2 additive after sintering at temperatures of 1250-1300-1350 degrees Celsius and (b) cordierite-tialite and cordierite-tialite containing magnesium additive after sintering at a temperature of 1300 degrees Celsius.

[DOI: 10.22068/ijmse.3659]